New Phytologist

A unique invertase is important for sugar absorption of an obligate biotrophic pathogen during infection

Qing Chang[1]*, Jie Liu[2]*, Xiaohong Lin[1], Shoujun Hu[2], Yang Yang[2], Dan Li[2], Liyang Chen[2], Baoyu Huai[2], Lili Huang[1], Ralf T. Voegele[3] and Zhensheng Kang[1,4]

[1]College of Plant Protection, State Key Laboratory of Crop Stress Biology for Arid Areas, Northwest A&F University, Yangling, 712100 Shaanxi, China; [2]College of Life Sciences, State Key Laboratory of Crop Stress Biology for Arid Areas, Northwest A&F University, Yangling, 712100 Shaanxi, China; [3]Fachgebiet Phytopathologie, Institut für Phytomedizin, Fakultät Agrarwissenschaften, Universität Hohenheim, 70593 Stuttgart, Germany; [4]China–Australia Joint Research Centre for Abiotic and Biotic Stress Management, Northwest A&F University, Yangling, 712100 Shaanxi, China

Author for correspondence:
Zhensheng Kang
Tel: +86 29 87091312
Email: kangzs@nwafu.edu.cn

Received: *27 March 2017*
Accepted: *17 May 2017*

New Phytologist (2017) **215:** 1548–1561
doi: 10.1111/nph.14666

Key words: host-induced gene silencing (HIGS), invertase, *Puccinia striiformis* f. sp. *tritici*, sucrose metabolism, sugar absorption.

Summary

- An increased invertase activity in infected plant tissue has been observed in many plant–pathogen interactions. However, the origin of this increased invertase activity (plant and/or pathogen) is still under debate. In addition, the role of pathogen invertases in the infection process is also unclear.
- We identified and cloned a gene with homology to invertases from *Puccinia striiformis* f. sp. *tritici* (*Pst*). Transcript levels of *PsINV* were analyzed by quantitative reverse transcription PCR in both compatible and incompatible *Pst*–wheat interactions . Function of the gene product was confirmed by heterologous expression, and its function in *Pst* infection was analyzed by host-induced gene silencing (HIGS).
- *Pst* abundantly secretes invertase during its invasion attempts whether in a compatible or incompatible interaction with wheat. Further research into the different domains of this protein indicated that the rust-specific sequence contributes to a higher efficiency of sucrose hydrolysis. With *PsINV* silenced by HIGS during the infection process, growth of *Pst* is inhibited and conidial fructification incomplete. Finally, pathogenicity of *Pst* is impaired and spore yield significantly reduced.
- Our results clearly demonstrate that this *Pst* invertase plays a pivotal role in this plant–pathogen interaction probably by boosting sucrose hydrolysis to secure the pathogen's sugar absorption.

Introduction

Sucrose and its decomposition products play essential roles in many processes throughout a plant's life cycle; not only do they serve as nutrients but also as signaling molecules (Smeekens *et al.*, 2010; Moghaddam & Ende, 2012; Ruan, 2012). As sucrose is also able to induce expression of defense-related genes in rice, it seems to be engaged in plant defense responses (Gómez-Ariza *et al.*, 2007). Sucrose is the major carbohydrate transported from source to sink tissue, and as such is also readily accessible to pathogens (Koch, 2004; Doidy *et al.*, 2012). Pathogens have developed different strategies to compete with their hosts for sucrose. *Ustilago maydis*, for example, has been reported to utilize the sucrose transporter *UmSRT1*, which exhibits a higher affinity than host sucrose transporters (Wahl *et al.*, 2010). In *Uromyces fabae* on the other hand, sucrose has to be first hydrolyzed to hexoses which are then taken up by the fungus through a hexose transporter (Voegele & Mendgen, 2011). Invertases (β-D-fructofuranoside fructohydrolase, EC 3.2.1.26), which irreversibly hydrolyze sucrose to glucose and fructose, are key enzymes in such processes. Much attention has been paid to invertases in plant–pathogen interactions, as it has been shown that invertase activity increased significantly in infected tissue (Long *et al.*, 1975; Scholes *et al.*, 1994; Tang *et al.*, 1996). Many studies have focused on the roles of plant invertases (Roitsch *et al.*, 2003; Roitsch & González, 2004; Siemens *et al.*, 2011). For example, in the powdery mildew and barley pathosystem, increased apoplastic invertase activity was found to be correlated with a higher degree of resistance (Swarbrick *et al.*, 2006). In tobacco repression of a cell wall invertase by RNA interference (RNAi) seems to have a positive effect on invasion and colonization by *Phytophthora nicotianae* (Essmann *et al.*, 2008). These results suggest that the increase of host invertase activity is part of the host defense system. However, given that invertases are also widely distributed among bacteria and fungi, it does not seem appropriate to conclude that only plant

*These authors contributed equally to this work.

© 2017 The Authors
New Phytologist © 2017 New Phytologist Trust

invertases contribute to the increase in invertase activity in all pathosystems. Especially with obligate biotrophic pathogens it is hard to discriminate between host and pathogen contributions to the overall activity (Doidy *et al.*, 2012; Lemoine *et al.*, 2013).

Although evolutionary reconstruction of the invertase gene family in numerous fungal phyla has revealed the presence of invertase-encoding genes in all sequenced pathogens (Parrent *et al.*, 2009), there are only a few studies which have investigated invertases from pathogenic fungi (Ruffner *et al.*, 1992; Ruiz & Ruffner, 2002; Voegele *et al.*, 2006). Research carried out on *Botrytis cinerea* showed that fungal invertase made a substantial contribution to the increase in invertase activity in infected grape tissue (Ruiz & Ruffner, 2002). Voegele *et al.* (2006) analyzed an invertase from *U. fabae*, and the high activity of this pathogen invertase suggested it could play a role in the observed increase in invertase activity. Although pathogen invertases have been reported to contribute to the increase in invertase activity, the biological function of these pathogen invertases in plant–pathogen interactions is still unclear.

Puccinia striiformis f. sp. *tritici* (*Pst*) is the causal agent of wheat stripe rust, one of the most widespread and destructive wheat diseases (Wellings, 2011). *Pst* is an obligate biotrophic pathogen and therefore its nutritional demands rely solely on living host tissue. As carbon sources are crucial for all organisms, it was of great interest to us how the pathogen secures its demand for carbon. In a previous study, it had been shown that sucrose accumulated in wheat leaves infected by *Pst* (Chang *et al.*, 2013). Sequence analyses showed there is no sucrose transporter present in *Pst*, only hexose transporters (Cantu *et al.*, 2011; Zheng *et al.*, 2013). Thus, it appears that *Pst* uses hexoses hydrolyzed from host sucrose to meet its own carbon demands. Invertases are therefore of great importance for this fungus. However, researchers were not sure whether the host or the pathogen invertase contributed more to the decomposition of host sucrose (Doidy *et al.*, 2012). Although it seems unlikely that the nutritional demands of the pathogen can be solely supported by the host's enzymatic machinery (Guenther *et al.*, 2009; Voegele & Mendgen, 2011), there is still no direct evidence for the significance of pathogen invertases in plant–pathogen interactions.

In this study, we cloned a gene with high similarity to invertase genes from *Pst*. This gene, *PsINV*, is highly conserved in different races of *Pst*. Phylogenetic analysis showed it has a unique, rust fungi-specific structure of conserved domains. The transcript profile of this gene was analyzed during *Pst* infection in both compatible and incompatible systems. Heterologous expression and complementation confirmed that this gene encodes an invertase. Enzymatic properties of *PsINV* were assayed with active protein purified from *Pichia pastoris*. As rust fungi-specific sequences were found in this invertase, the functions of different domains were further investigated. Finally, silencing of *PsINV* limited fungal growth and also had a detrimental effect on sporulation. This study is the first to directly reveal the significance of a pathogen invertase.

Materials and Methods

Cultivation of plants and micro-organisms

Seedlings of wheat cultivars Suwon 11 and 92R137 were inoculated with urediospores of the currently prevalent *Pst* races CYR31 and CYR32 (Chen *et al.*, 2009; Zhang *et al.*, 2013). Suwon 11 produced compatible reactions with CYR31 and CYR32, whereas 92R137 produced incompatible reactions with CYR31 and CYR32. In addition, CYR23 and CYR25, two *Pst* races prevalent in the past, were inoculated on wheat cultivars MingXian 169 (compatible) and Suwon 11 (incompatible). Fresh urediospores were obtained from infected wheat leaves. After inoculation, samples of compatible and incompatible systems were taken independently at different time points, up to 264 h post inoculation (hpi). Three independently inoculated leaves were combined in one sample. For quantitative reverse transcription PCR (qRT-PCR) analyses, three independent biological replicates were performed for each *Pst* race on both compatible and incompatible systems.

Escherichia coli strain TOP10 was grown in Luria–Bertani medium supplemented with the pertinent concentration of antibiotic for plasmid maintenance. *Saccharomyces cerevisiae* strains YTK12 and SEY2102 were cultured in yeast-potato-dextrose (YPD) medium at 30°C. *P. pastoris* strain GS115 was also grown at 30°C in YPD medium.

Isolation of RNA and sequence analysis

Total RNA from urediospores was extracted using TRIzol reagent (Invitrogen) following the manufacturer's instructions. After digestion with DNase I, RNA was reverse-transcribed into cDNA using MMLV reverse transcriptase (Promega). One of the expressed sequence tags (ESTs) from a full-length cDNA library of *Pst* previously constructed in our laboratory showed high similarity to the invertase gene *Uf-INV1* from *U. fabae* (GenBank accession number CAG26671). The open reading frame (ORF) of *PsINV* was cloned from first-stand cDNA with specific primers PsINV-F and PsINV-R, which were designed based on the EST sequence (Supporting Information Table S1) (Zhang *et al.*, 2008).

The complete sequence of this gene was obtained from the publicly available genome of *Pst* downloaded from the NCBI genome database (http://www.ncbi.nlm.nih.gov/genome/). The nucleotide sequences of different races were aligned with CLUSTALW to analyze potential polymorphisms (Thompson *et al.*, 1994). Protein sequences with homology to the amino acid sequence of *Ps*INV in a set of fungal genomes were obtained by database searches using BLASTP (http://www.ncbi.nlm.nih.gov/; http://www.broadinstitute.org/). In addition, invertase sequences from wheat were also used for building the phylogenetic tree. Multiple alignments were performed using CLUSTALW, and the phylogenetic tree was reconstructed using MEGA5 software (Tamura *et al.*, 2011). Physicochemical properties of the predicted protein were determined using the PROTPARAM tool on the ExPASy server (http://www.expasy.org). The deduced amino acid

© 2017 The Authors
New Phytologist © 2017 New Phytologist Trust

sequences of *Ps*INV and other invertases were analyzed using PFAM (http://pfam.xfam.org/) for conserved domains and motifs (Finn *et al.*, 2016). The deduced amino acid sequence of *Ps*INV was submitted to PHYRE2 (http://www.sbg.bio.ic.ac.uk/phyre2/) for three-dimensional (3D) molecular model prediction by homology modeling (Kelley *et al.*, 2015). PYMOL (Schrödinger Inc., New York, NY, USA) was used to recolor the developed 3D structural model of *Ps*INV. SIGNALP 4.1 (http://www.cbs.dtu.dk/services/SignalP/) and PHOBIUS (http://phobius.sbc.su.se/) were used for prediction of a signal peptide (Käll *et al.*, 2007; Petersen *et al.*, 2011).

qRT-PCR analysis

To analyze the transcript levels of *PsINV*, relative quantification of gene expression was performed using qRT-PCR on an ABI Prism 7500 real-time PCR system (Applied Biosystems). Specific primers for the target and reference genes were designed using Primer PREMIER 5.0 (Table S1). Real-time PCR was performed with 12.5 μl 2 × SYBR Premix Ex Taq (TaKaRa, Tokyo, Japan), 9.0 μl distilled H_2O, 0.5 μl ROX Reference Dye II, 1.0 μl cDNA template, 1 μl forward primer (10 mM) and 1 μl reverse primer (10 mM) in a total reaction volume of 25 μl. The reaction conditions were as follows: 95°C for 1 min, and 40 cycles of 95°C for 10 s, 60°C for 20 s and 72°C for 36 s. Each reaction was carried out in triplicate and included three nontemplate controls. The specificity of the amplicon was confirmed by using the ABI Prism Dissociation Curve Analysis software after the PCR. Real-time PCR data were analyzed using the comparative $2^{-\Delta\Delta CT}$ method to quantify relative gene expression (Livak & Schmittgen, 2001). Two parameters, a relative amount of RNA of at least threefold higher or lower than controls and a *P*-value < 0.01, were used to assess differences between time points.

Nucleic acid manipulations

To check whether *Ps*INV is secreted or not, the sequence encoding the signal peptide was cloned using primers INVS-F and INVS-R with *Eco*RI and *Xho*I. The signal peptide sequence was then inserted into digested pSUC2 vector.

To construct plasmid *PsINV*::pDR195 for heterologous expression, full-length *PsINV* was amplified using a pair of primers with *Not*I and *Bam*HI restriction sites: INV-F and INV-R. The amplified fragment was digested with *Not*I and *Bam*HI and ligated into vector pDR195 digested with the same enzymes. For expression of *PsINV* in *P. pastoris*, another reverse primer, INVexp-R, carrying an *Xba*I restriction site, was used along with INV-F to amplify the ORF of *PsINV*. The PCR product was digested with *Not*I and *Xba*I and inserted into the digested vector pPICZα-A.

Different domains of *Ps*INV protein were deleted by overlapping PCR with four pairs of internal primers, PsINVΔN-F/PsINVΔN-R, PsINVΔN1-F/PsINVΔN1-R, PsINVΔN2-F/PsINVΔN2-R and PsINVΔC-F/PsINVΔC-R, which were all designed by Primer PREMIER 5.0. Different fragments were first obtained with PCR using PsINV-F and PsINV-R separately with these primers, and fragments *PsINVΔN*, *PsINVΔN1*, *PsINVΔN2* and *PsINVΔC* were then obtained by overlapping PCR with these fragments.

Barley stripe mosaic virus-host-induced gene silencing (BSMV-HIGS) vectors were generated as described (Holzberg *et al.*, 2002). Three cDNA fragments were chosen from the ORF of *PsINV* based on results of a BLASTN search in the NCBI database showing that these three fragments had no other similar sequences. The target fragments were amplified by PCR using primer pairs PsINV1asF/PsINV1asR, PsINV2asF/PsINV2asR and PsINV3asF/PsINV3asR with *Not*I and *Pac*I restriction sites, respectively . Amplicons were ligated into the BSMV:γ vector to generate recombinant plasmids BSMV:PsINV1as, BSMV:PsINV2as and BSMV:PsINV3as. The empty BSMV:γ vector (BSMV:00) was used as negative control. Primers for all plasmid constructs are listed in Table S1.

Functional validation of the signal peptide

To confirm the function of the identified signal peptide of *Ps*INV, a yeast secretion system was established. The recombinant vector *PsINVS*::pSUC2 was transformed into the yeast strain YTK12 using the lithium acetate method. In this experiment, the signal peptides of Avr1b and *Ps*87 were used as positive controls, and the sequence encoding the first 25 amino acids of *Mg*87 was used as a negative control. *Avr1b*::pSUC2 and *Ps87*::pSUC2 were also transformed into YTK12 cells as positive controls, and *Mg87*::pSUC2 and the empty vector pSUC2 were transformed into YTK12 cells as negative controls (Gu *et al.*, 2011). After transformation with these pSUC2 vectors, the transformed YTK12 strains were inoculated on CMD-W medium (0.67% yeast nitrogen base (YNB) without amino acids, 0.075% tryptophan dropout supplement, 2% sucrose, 0.1% glucose and 2% agar) and YPRAA medium (1% yeast extract, 2% peptone, 2% raffinose, 2 mg ml^{-1} antimycin A and 2% agar) at equivalent concentrations.

Complementation of the invertase-deficient yeast strain

To identify the function of *Ps*INV, the invertase-deficient yeast strain SEY2102 was transformed with the heterologous expression vector *PsINV*::pDR195 using electroporation. Transformants were selected on synthetic complete (SC) medium lacking uracil with 2% glucose at 30°C. After confirmation of *PsINV* in the transformants by PCR analysis, transformants were cultured in SC medium lacking uracil with 2% sucrose as sole carbon source. Transformants with the empty vector pDR195 were used as negative control.

Expression and purification of His-tagged fusion proteins

The eukaryotic expression plasmid *PsINV*::pPICZα-A was linearized with *Pme*I before transformation into *P. pastoris* GS115. The transformant with the largest number of recombinant plasmids integrated into the fungal genome was chosen by antibiotic

© 2017 The Authors
New Phytologist © 2017 New Phytologist Trust

screening. The transformant was first cultured in BMGY (1% yeast extract, 2% peptone, 100 mM potassium phosphate pH 6.0, 1.34% YNB without amino acids, 4×10^{-5}% biotin, 1% glycerol) for 2 d for propagation and was then cultured in BMMY (1% yeast extract, 2% peptone, 100 mM potassium phosphate pH 6.0, 1.34% YNB, 4×10^{-5}% biotin, 0.5% methanol) to induce expression of the protein. The culture medium was sampled every 24 h for 120 h.

His-tagged protein was purified from the supernatant on a column containing Ni-NTA resin (GenScript, Jiangning, China). The column was first washed with five volumes of wash buffer (50 mM NaH_2PO_4, 300 mM NaCl, 20 mM imidazole, pH 7.2) and then eluted in 2 ml fractions with elution buffer (50 mM NaH_2PO_4, 300 mM NaCl, 300 mM imidazole, pH 7.2).

Domain function analysis

Primers INV-F and INV-R were used to amplify knockout fragments, *PsINVΔN*, *PsINVΔN1*, *PsINVΔN2* and *PsINVΔC*, and to append restriction sites to these fragments. These fragments were recombined into the heterologous expression vector pDR195 for transformation into yeast strain SEY2102. At the same time, these fragments were cloned into the eukaryotic expression vector pPICZα-A with primers INV-F and INVexp-R for eukaryotic expression. All transformants were checked by PCR analysis.

Enzyme assays

Proteins expressed in the *P. pastoris* expression system (*Ps*INV, *Ps*INVΔN, *Ps*INVΔN1, *Ps*INVΔN2 and *Ps*INVΔC) were stored in culture filtrate at 4°C. Invertase activities were measured in reaction mixtures containing the enzyme, 100 mM sodium acetate buffer (pH 4.6) and 100 mM sucrose solution, and the reactions were incubated for 10 min at 35°C. The reaction was stopped by addition of 1 ml 0.5 M NaOH, thus shifting the pH far into the alkaline range. DNS reagent (10.6 g 3,5-dinitrosalicylic acid, 306 g sodium potassium tartrate, 7.6 ml phenol crystals and 8.3 g sodium metabisulfite dissolved in 1416 ml of distilled water), as recommended by The International Union of Pure and Applied Chemistry was then added to the mixture (Ghose, 1987). After incubation for 10 min in boiling water and subsequent cooling to 25°C, the color intensity at 560 nm was determined (Miller, 1959). The optimum temperature was determined by varying the incubation temperature at constant pH. The optimum pH was determined using Na-acetate and phosphate buffers at the indicated pH values at 35°C. Kinetic analysis was performed by varying the sucrose concentration, and the K_m was calculated by the Lineweaver–Burk method (Price, 1985). Different divalent metal ions and EDTA were added to the standard assay at 5 mM to determine their effects on invertase activity. Protein concentrations were quantified according to Bradford following the microassay procedure with dilutions of BSA as standards (Bradford, 1976). All assays were performed in triplicate and repeated at least twice.

BSMV-mediated silencing of *PsINV*

Suwon 11 wheat seedlings were grown in a soil mixture (Quanhui Fertilizer Co., Ltd, Shandong, China) in 10 cm diameter pots in a growth chamber at 16°C with 60% relative humidity and a 16 h photoperiod (60 μmol m^{-2} s^{-1}) to the two-leaf stage. Capped transcripts were prepared from the linearized plasmids containing the tripartite BSMV genome using the mMESSAGE T7 *in vitro* transcription kit (Ambion). The BSMV transcripts were then inoculated with 1 × FES buffer onto the second leaf of the wheat seedlings by rubbing with gloved fingers. Three independent sets of plants were inoculated for each of the BSMV viruses (BSMV:00, BSMV:PsINV1as, BSMV:PsINV2as, BSMV:PsINV3as). Plants inoculated with BSMV:TaPDSas, which encodes the *Triticum aestivum* phytoene desaturase, were used as positive controls. Plants inoculated with another silencing construct, BSMV:PsSRPKLas, which had been reported to be able to silence a *Pst* protein kinase gene to have an effect on *Pst* pathogenicity, were also used as positive controls (Cheng *et al.*, 2015). As negative controls, wheat seedlings were mock inoculated with only 1 × FES buffer. After growth for 10 d in a chamber at 25°C, the phenotypes were observed and photographs were taken of the fourth leaves of the plants inoculated with virus. Fourth leaves were then inoculated with fresh urediospores from the *Pst* pathotype CYR32. The fourth leaves were sampled at 24, 48, 120 and 168 hpi for qRT-PCR and histological observation. Finally, at 14 d post-inoculation (dpi), the *Pst* infection phenotypes were recorded and photographed. DNA from the infected leaves was then extracted for measuring the biomass changes using absolute quantification by qRT-PCR (Li *et al.*, 2011). The standard curves for wheat and *Pst* were established with the recombinant plasmids carrying either *TaEF* or *PsEF1* (Liu *et al.*, 2015). Numbers of gene copies were calculated using the gene-specific standard curves for wheat and *Pst*. The biomass ratio was acquired by comparing the *PsEF1* copy numbers with *TaEF* copy numbers. All primers are listed in Table S1.

Histological observation of fungal growth

To determine the effect of silencing *PsINV* on *Pst* growth histologically, sampled leaves were first fixed and decolorized in ethanol/trichloromethane (3 : 1, v/v) for 3–5 d. After staining with wheat germ agglutinin (WGA) conjugated to Alexa-488 (Invitrogen), the infected leaves were examined with an Olympus BX-51 microscope (Olympus Corp., Tokyo, Japan) to observe the number of hyphal branches, the length of the hyphae and the infection areas under ultraviolet light (excitation wavelength 450–480 nm, emission wavelength 515 nm) (Hood & Shew, 1996; Wang *et al.*, 2007). For each sample and its biological replicate, the data of 50 infection sites from five randomly selected leaves were recorded. Only a site where a substomatal vesicle formed was considered an infection site. The data were analyzed with the SAS software package (SAS Institute, Cary, NC, USA) using a one-way ANOVA test. Differences were considered significant at a probability level of $P < 0.01$.

© 2017 The Authors
New Phytologist © 2017 New Phytologist Trust

Results

PsINV has a rust fungi-specific structure

The full-length ORF of *PsINV* was cloned from the cDNA of CYR32 urediospore germlings with specific primers. The ORF of *PsINV* comprised 2310 bp, encoding a protein of 769 amino acids. Sequence data for *PsINV* have been deposited at GenBank under accession number KX230123. The molecular weight of the predicted protein was 86.66 kDa, and the theoretical pI of the predicted protein was 6.37. By comparing the nucleotide sequences of *PsINV* from seven *Pst* isolates whose genomes have been publicly available on the NCBI genome database, it was shown that this gene was highly conserved in all *Pst* races with no more than three nucleotide substitutions (Fig. S1).

The 769 amino acids sequence of *Ps*INV was used as a query to search protein databases. Invertases from both nonpathogenic fungi and pathogenic fungi showing high similarity to *Ps*INV were identified. A phylogenetic tree was reconstructed with a total of 56 fungal and four wheat invertases. The phylogenetic analysis revealed that *Ps*INV clustered with other rust invertases in one clade (Fig. 1a). The results of domain prediction analysis showed that *Ps*INV has two glycosyl hydrolase family 32 N-terminal domains, named N1 and N2, and one glycosyl hydrolase family 32 C-terminal domain, named C domain, according to the Pfam protein families database. The N domain was the combination of two (N1 and N2) domains. In contrast to invertases of yeast and some other pathogenic fungi, this has one N-terminal domain and one C-terminal domain (Fig. 1b). PHYRE2 was used to construct a 3D molecular model of *Ps*INV by

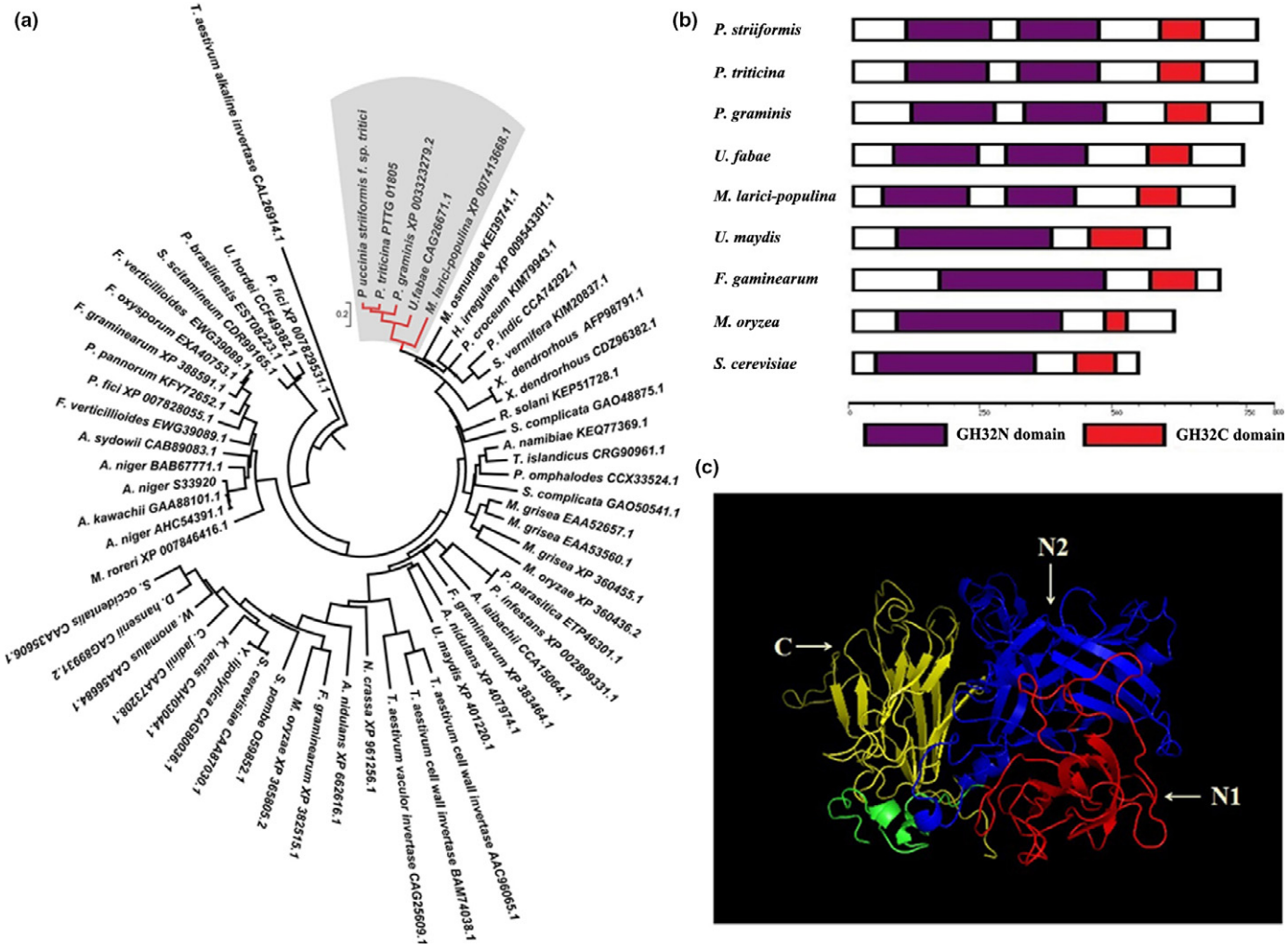

Fig. 1 Phylogenetic analysis and bioinformatic predictions for *Ps*INV. (a) Phylogenetic analysis of *Ps*INV from *Puccinia striiformis* f. sp. *tritici* and other fungal invertases carried out using the neighbor-joining method. The shaded area indicates invertases from rust fungi. (b) Domain analysis using Pfam. Three domains were identified, and the predicted regions of the three domains were from residue 99 to 273, 299 to 475 and 582 to 667, termed the N1 domain, N2 domain and C domain, respectively. The N domain was defined as a combination of N1 and N2 domains (from residue 99 to 475). All rust invertases (*P. striiformis*, *Puccinia striiformis* f. sp. *tritici*; *P. triticina*, *Puccinia triticina*; *P. graminis*, *Puccinia graminis* f. sp. *tritici*; *U. fabae*, *Uromyces fabae*; *M. larici-populina*, *Melampsora larici-populina*) show a similar structure, different from invertases from other fungi (*U. maydis*, *Ustilago maydis*; *F. graminearum*, *Fusarium graminearum*; *M. oryzae*, *Magnaporthe oryzae*; *S. cerevisiae*, *Saccharomyces cerevisiae*). (c) 3D molecular model of *Ps*INV constructed using PHYRE2.

© 2017 The Authors
New Phytologist © 2017 New Phytologist Trust

homology modeling methods (Kelley *et al.*, 2015), and different colors were used to label the different domains with PyMOL (Fig. 1c).

Functional validation of the signal peptide of *Ps*INV

To determine whether *Ps*INV is secreted into the host tissues, several bioinformatic prediction websites were used to clarify whether *Ps*INV has a signal peptide. Although no signal peptide was identified by SignalP 4.1, Phobius showed there was a signal peptide composed of 60 amino acids encoded by the first 180 bp of *PsINV*. The signal peptide of *Ps*INV was cloned into the pSUC2 vector for further verification. With both positive controls and negative controls, the transformed yeast strains were inoculated on both CMD-W medium and YPRAA medium for functional testing. It was shown that the signal peptide of *Ps*INV had the same effect on secretion of SUC2 as well-known signal peptides from fungi, including *Pst* (Fig. 2) (Gu *et al.*, 2011). This result confirmed the presence of a functional signal peptide in *Ps*INV.

Transcript profiles of *PsINV*

To gain insight into a possible function of *PsINV* during *Pst* infection, we analyzed transcript abundance of *PsINV* at different time points during the infection process by qRT-PCR. As changes in sugar levels were observed in both compatible and incompatible systems in a previous report (Chang *et al.*, 2013), transcript profiles of *PsINV* were analyzed in the two systems. In incompatible systems, *Pst* could grow sustainably with growth limitation before obvious necrosis appeared on infected leaves 13–15 dpi (Fig. S2). Samples were collected for both compatible and incompatible systems up to 264 hpi when new spores are produced in the compatible systems. With quantification of *PsINV* expression profiles in different compatible and incompatible systems inoculated with different *Pst* races, all results show a similar expression pattern. In compatible systems, the expression of *PsINV* is induced at the beginning of the infection process. At 72–168 hpi, transcript levels increased sharply as secondary hyphae extended and numerous haustoria formed (Fig. 3). Expression then decreased to very low levels. In incompatible systems, a similar expression pattern as in compatible systems was observed before 168 hpi, but the decline of this expression was much slower than that in the compatible systems after 168 hpi. The abundance of *PsINV* transcripts during the infection process suggests that *PsINV* plays an important role in *Pst* infection.

Heterologous expression of *PsINV*

To characterize *Ps*INV in *S. cerevisiae*, the complete ORF was cloned into *S. cerevisiae* expression vector pDR195. Transformants of *S. cerevisiae* strain SEY2102 were obtained by transformation with either the empty vector pDR195 or the recombinant plasmid pDR195::*PsINV*. Both types of transformants show no difference in growth on SC medium with glucose as carbon source (Sherman, 1991). However, on SC medium with sucrose as sole carbon source, pDR195 transformants could not grow at all, but pDR195::*PsINV* transformants could complement the invertase-negative phenotype of this strain (Fig. 4a). This result confirms that *Ps*INV acts as an invertase *in vivo*.

To confirm that *Ps*INV acts as a true invertase *in vitro*, vector pPICZαA::*PsINV* was constructed for expression of *PsINV* in *P. pastoris*. With an alpha factor signal added to the N terminus of *Ps*INV, the mature protein is secreted into the culture medium. The transformant with the largest number of

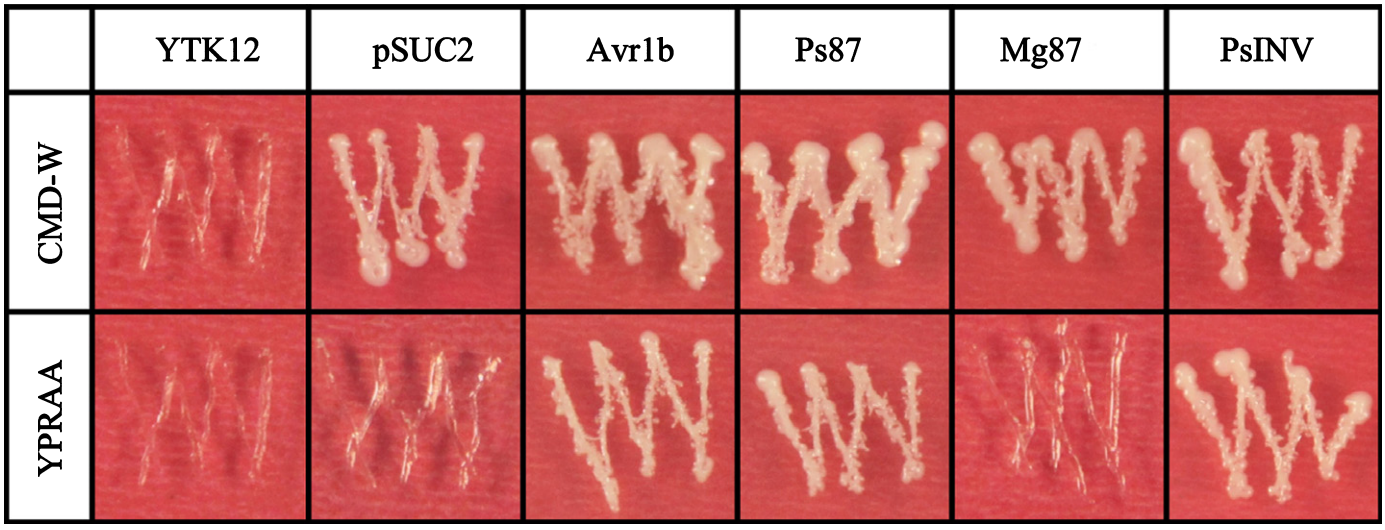

Fig. 2 Functional validation of the signal peptide of *Ps*INV. Signal peptides of Ps87 from *Puccinia striiformis* f. sp. *tritici* and Avr1b from *Phytophthora sojae* were cloned into pSUC2 as positive controls. Untransformed *Saccharomyces cerevisiae* strain YTK12, and YTK12 carrying the empty pSUC2 vector defined as pSUC2 were used as negative controls. The first 25 amino acids of Mg87 (no signal peptide function) from *Magnaporthe oryzae* were also used as negative control. CMD-W, medium with 0.67% yeast nitrogen base (YNB) without amino acids, 0.075% tryptophan dropout supplement, 2% sucrose, 0.1% glucose and 2% agar; YPRAA, medium with 1% yeast extract, 2% peptone, 2% raffinose, 2 mg ml^{-1} antimycin A and 2% agar.

© 2017 The Authors
New Phytologist © 2017 New Phytologist Trust

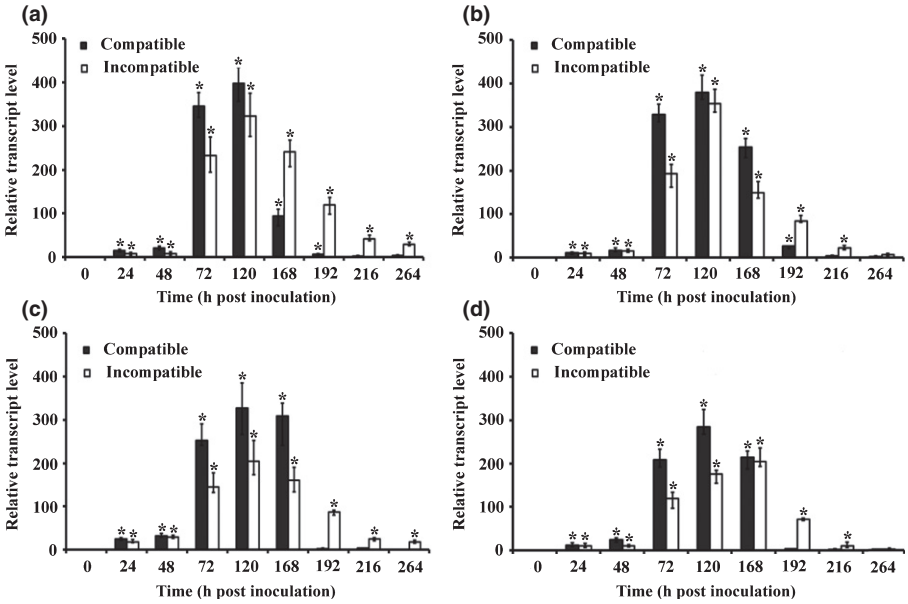

Fig. 3 Transcript profiles of *PsINV*. Relative transcript levels of *PsINV* from *Puccinia striiformis* f. sp. *tritici* were analyzed with four different *Pst* races (CYR32, CYR31, CYR25, CYR23) in both compatible and incompatible systems. (a) CYR32 was inoculated on Suwon 11 (*Triticum aestivum*) as compatible system and 92R137 (*T. aestivum*) as incompatible system. (b) CYR31 was inoculated on Suwon 11 as compatible system and 92R137 as incompatible system. (c) CYR25 was inoculated on Mingxian 169 (*T. aestivum*) as compatible system and Suwon 11 as incompatible system. (d) CYR23 was inoculated on Mingxian 169 as compatible system and Suwon 11 as incompatible system. Bars indicate means of three independent biological replicates (± SE). Asterisks indicate a significant difference ($P < 0.01$) between different time points.

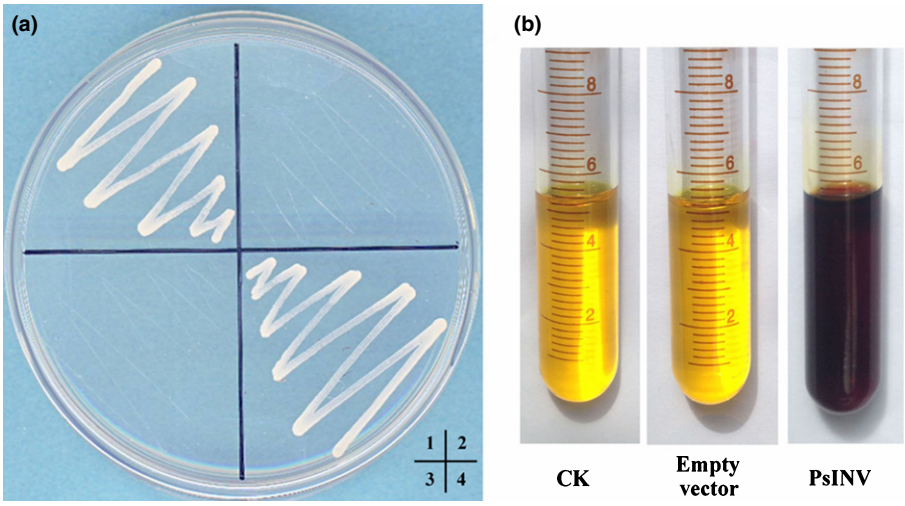

Fig. 4 Heterologous expression of *PsINV*. (a) The *ΔINV Saccharomyces cerevisiae* strain SEY2102 was complemented with pDR195::*PsINV* on synthetic complete (SC) media with sucrose as the sole carbon source. 1, wild type *S. cerevisiae*; 2, SEY2102; 3, SEY2102 transformed with pDR195; 4, SEY2102 transformed with pDR195::*PsINV*. (b) Culture filtrate of *Pichia pastoris* GS115 transformed with the empty vector pPICZαA or the vector carrying *PsINV* was used to confirm invertase activity by the DNS colorimetric method. Culture medium (CK) was used as negative control.

recombinant plasmids integrated into the fungal genome was chosen for induced expression of *Ps*INV protein. The largest quantity of the expressed protein was detected in the cell-free culture filtrates at 120 h post-induction. Western blot analysis of the recombinant protein confirmed that the target protein is expressed (Fig. S3). Enzyme activity was detected by hydrolysis of sucrose with the soluble *Ps*INV *in vitro*. Using the DNS colorimetric method, sucrose was shown to be hydrolyzed into reducing sugars (Fig. 4b). This result further confirms that *Ps*INV is a true invertase and suggests that the expressed protein can be utilized for further biochemical characterization.

Enzymatic characterization of *Ps*INV

Enzymatic characterizations of *Ps*INV were performed with purified *Ps*INV protein. By changing the incubation temperature, it was shown that the optimum temperature of *Ps*INV is *c.* 40°C (Fig. 5a). The optimum pH was confirmed to be slightly below pH 5.0 (Fig. 5b). The Michaelis–Menten kinetics of the enzyme was determined using the Lineweaver–Burk method. The K_m was determined to be 19.92 mM under optimal conditions (Fig. 5c). In addition, the effects of different divalent metal ions and EDTA were tested independently (Fig. 5d). Zinc and ferrous ions had no effect on enzyme activity. By contrast, copper ions inhibited the enzyme activity significantly and could even completely suppress activity. However, manganese ions enhanced enzyme activity twofold. Addition of EDTA resulted in a decrease in enzyme activity. This suggests that manganese ions may be a cofactor of this invertase.

Functional analysis of different domains

As described earlier, a rust fungi-specific sequence was discovered in this gene. Therefore, further research into the functions of each

© 2017 The Authors
New Phytologist © 2017 New Phytologist Trust

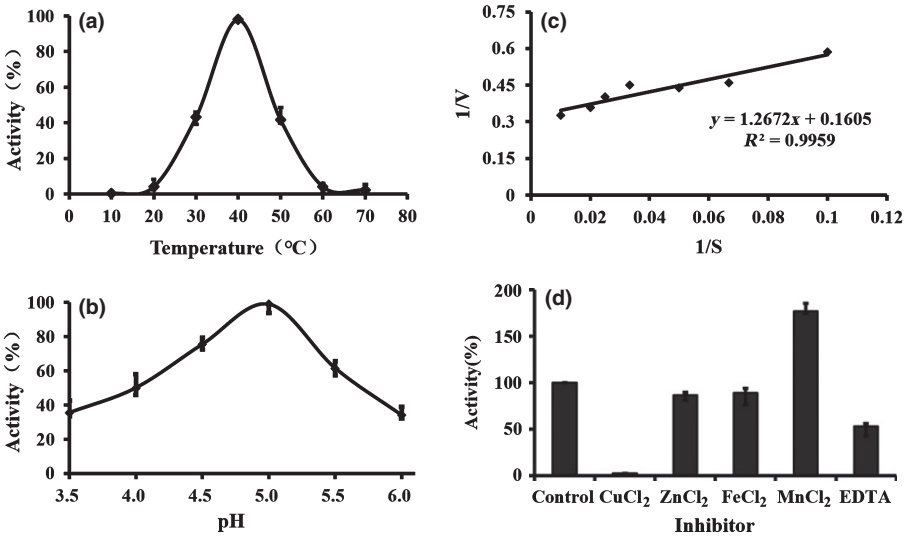

Fig. 5 Enzymatic characterization of *Ps*INV. With the *Ps*INV protein purified from eukaryotic expression products, the optimum temperature, optimum pH, K_m and the metal ion effects of this protein was analysed *in vitro*. (a) Optimum temperature was determined under standard conditions varying just the assay temperature. (b) Optimum pH was assayed using 100 mM Na-acetate, or 100 mM Na-phosphate buffer at 35°C. (c) Lineweaver–Burk plot for *Ps*INV. The K_m was calculated to 19.92 mM using a linear fit. (d) Cu^{2+} seems to have a negative effect on *Ps*INV activity, whereas Mn^{2+} ions showed the opposite effect. Bars represent the means of triplicate experiments ± SE. Asterisks indicate a significant difference ($P < 0.01$).

domain was conducted. Fragments with deletions of different domains were obtained and used for both heterologous expression and eukaryotic expression with the full gene as the positive control. With the heterologous expression system, it was shown that only *PsINVΔN1* could complement the invertase defect, but the transformant grew more slowly than the positive control (Fig. 6b). The proteins *Ps*INVΔN, *Ps*INVΔN1, *Ps*INVΔN2 and *Ps*INVΔC expressed by heterologous expression were tested for invertase activity as described earlier (Fig. S4). *Ps*INVΔN, *Ps*INVΔN2 and *Ps*INVΔC had no activity, whereas *Ps*INVΔN1 was active but had lower activity than *Ps*INV (Fig. 6a). Taken together, these results indicate that the N2 domain and C domain are required for invertase activity, whereas the N1 domain seems to regulate the invertase activity level.

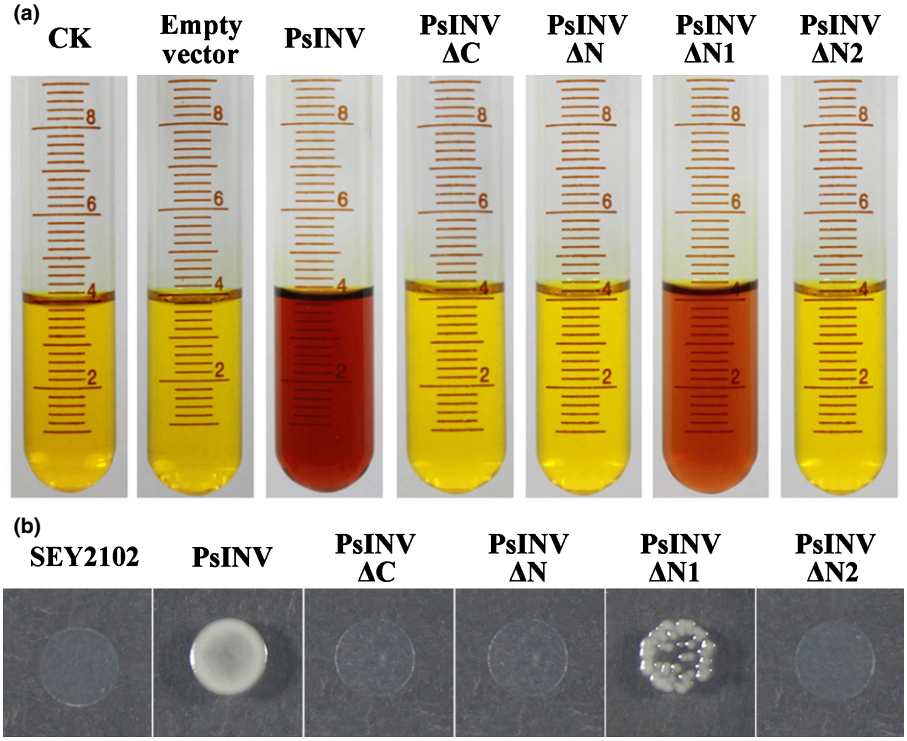

Fig. 6 Functional analysis of different *Ps*INV mutants. (a) Invertase activity assay (DNS colorimetric method) on full *Ps*INV (positive control) and several deletion mutant proteins (*Ps*INVΔC, *Ps*INVΔN, *Ps*INVΔN1 and *Ps*INVΔN2 with C domain, both N1 and N2 domains, N1 domain, and N2 domain knocked out, respectively). Culture medium (CK) and culture filtrate of *Pichia pastoris* carrying the empty vector were used as negative controls. (b) Different *PsINV* deletion constructs (*Ps*INVΔC, *Ps*INVΔN, *Ps*INVΔN1 and *Ps*INVΔN2 with the fragments encoding C domain, both N1 and N2 domains, N1 domain, and N2 domain knocked out, respectively) were cloned into vector pDR195 for analysis in an SEY2102 (*Saccharomyces cerevisiae*) background. pDR195:: *PsINV* served as positive control. Untransformed SEY2102 was used as negative control.

© 2017 The Authors
New Phytologist © 2017 New Phytologist Trust

HIGS for *PsINV*

Due to the lack of a stable genetic transformation system for *Pst*, BSMV-induced RNAi of pathogen genes, termed HIGS, has been developed as a useful tool for studying the function of pathogenic genes by silencing gene expression and has been commonly used in biotrophic pathogens of cereals (Nowara *et al.*, 2010; Nirmala *et al.*, 2011; Panwar *et al.*, 2013; Cheng *et al.*, 2015). Three independent fragments of *PsINV* were designed for silencing the expression of this gene during the *Pst* infection process. The three fragments were selected to have no effect on expression of the wheat invertase genes with no more than 11 consecutive identical nucleotides observed between *PsINV* and all wheat invertase genes accessed on NCBI (Fig. S5) (Senthil-Kumar *et al.*, 2007). At 10 dpi with BSMV, plants inoculated with BSMV:00, BSMV:PsINV1as, BSMV:PsINV2as, BSMV:PsINV3as and BSMV:PsSRPKLas all displayed the same phenotype of mild chlorotic mosaic symptoms but showed no significant defects in wheat growth and development. However, plants inoculated with BSMV:TaPDSas showed severe symptoms of Chl photobleaching, suggesting that the BSMV-HIGS system worked well (Fig. 7a). With the plants inoculated with BSMV:00 as negative controls and the plants inoculated with BSMV:PsSRPKLas as positive controls, the rust disease phenotypes of the plants inoculated with *PsINV* silencing constructs were photographed at 14 dpi of fresh *Pst* CYR32 urediospores. A significant reduction in sporulation was observed on wheat leaves inoculated with the *PsINV* silencing constructs compared with leaves of the positive control (Fig. 7b). Counting uredia on infected leaves further supports this conclusion (Fig. 7c). The biomass of *Pst* also shows a decrease in

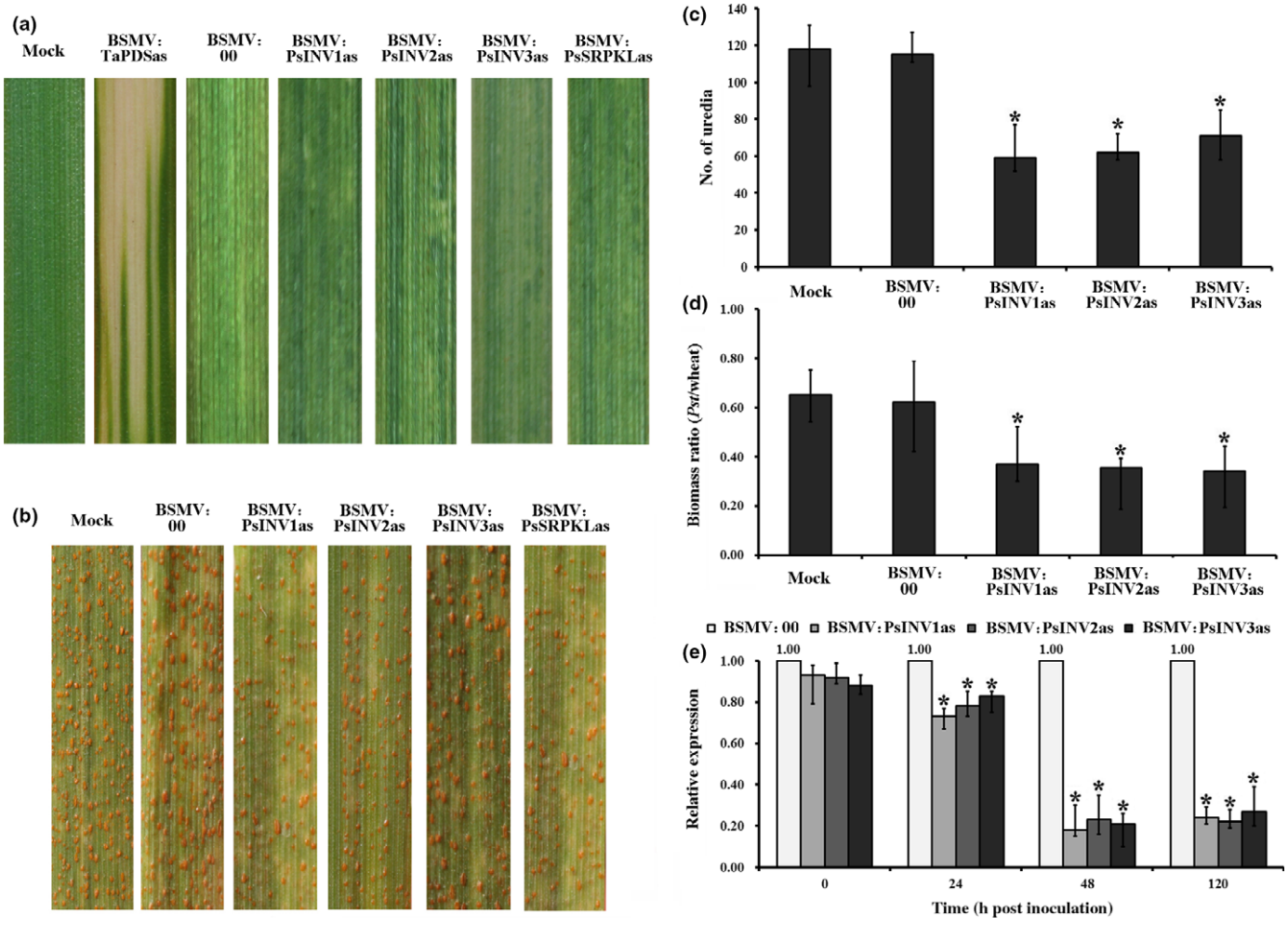

Fig. 7 Analysis of *PsINV* during infection of wheat using HIGS. (a) Mild chlorotic mosaic symptoms were observed on the fourth leaves of seedlings at 10 d post-inoculation (dpi) with BSMV:00, BSMV:PsINV1as, BSMV:PsINV2as, BSMV:PsINV3as and BSMV:PsSRPKL. Photobleaching was evident on fourth leaves of plants infected with BSMV:TaPDS. No change of phenotype was observed on the fourth leaves of mock-inoculated plants. (b) Disease phenotypes of the fourth leaves challenged with the virulent *Pst* isolate CYR32. BSMV:00 was the negative control and BSMV:PsSRPKL was the positive control. (c) Uredia density on silenced plants quantified 14 dpi. (d) Fungal and wheat biomass ratio measured via total DNA content at 14 dpi by absolute quantification using the internal reference genes *PsEF* and *TaEF*, respectively. (e) Silencing efficiencies were assessed by qRT-PCR. Values are expressed relative to the reference gene *PsEF*, with the empty vector (BSMV:00) set to 1. Values represent mean ± SE of three independent replicates. Differences were assessed using Student's *t*-tests. Asterisks indicate $P < 0.01$.

© 2017 The Authors
New Phytologist © 2017 New Phytologist Trust

PsINV-silenced plants (Figs 7d, S6). As the expression of *PsINV* was significantly reduced in *PsINV*-silenced plants (Fig. 7e), these results indicate that *Ps*INV seems to contribute to pathogenicity of *Pst* on wheat leaves.

Histological analysis of the effect of silencing *PsINV*

Cytological effects of silencing *PsINV* on *Pst* growth and development were determined at different infection stages at 24, 48, 120 and 168 hpi. In plants inoculated with the three *PsINV*-silencing constructs, no significant difference was observed in fungal development compared with in the plants inoculated with BSMV:00 at 24 hpi (Table S2). Secondary hyphae formed normally in control plants at 48 hpi, whereas growth of *Pst* lagged in *PsINV*-silenced plants as the primary hyphae were swollen and no secondary hyphae formed (Fig. 8). At 120 hpi, when many haustoria were formed, the infection areas of *Pst* in *PsINV*-silenced plants were much smaller than those in the control plants. In addition, the pustule bed matured imperfectly when *PsINV* was silenced at 7 dpi when the sporulation structure begins to form. The sporulation bed was undeveloped and unable to produce spores. This result suggests that silencing *PsINV* not only inhibits growth and development of *Pst* but also has strong effects on sporulation.

Discussion

As most pathogenic fungi are heterotrophic organisms that rely on their hosts to meet their carbon demands, water-soluble carbohydrates, especially sucrose, have been observed to be altered in infected leaves in many different pathosystems (Wright *et al.*, 1995; Chang *et al.*, 2013). Host sucrose alterations are believed to be due to the activity of plant cell-wall invertases (Roitsch & González, 2004; Hayes *et al.*, 2010). However, it is unknown if microbial invertase activities also play a role. In most pathosystems, especially with obligate biotrophic pathogens, it is difficult to discriminate between plant or pathogen contributions to the increased invertase activity (Doidy *et al.*, 2012; Lemoine *et al.*, 2013). In this study, we focused on an invertase gene from *Pst*, *PsINV*. The ORF of *PsINV* was cloned and showed a rust fungi-specific structure. Little variation was observed for this gene, indicating it could be a core gene with a pivotal role for *Pst*. The secretion and high level of expression of *Ps*INV indicates that *Pst* utilizes this invertase to aggressively hydrolyze host sucrose for its own carbon demands. Additionally, heterologous expression of this gene in both *S. cerevisiae* and *P. pastoris* confirmed the function of this gene as an invertase both *in vivo* and *in vitro*. Enzymatic characteristics of this invertase were determined with active purified *Ps*INV. Further analysis of the gene product showed that

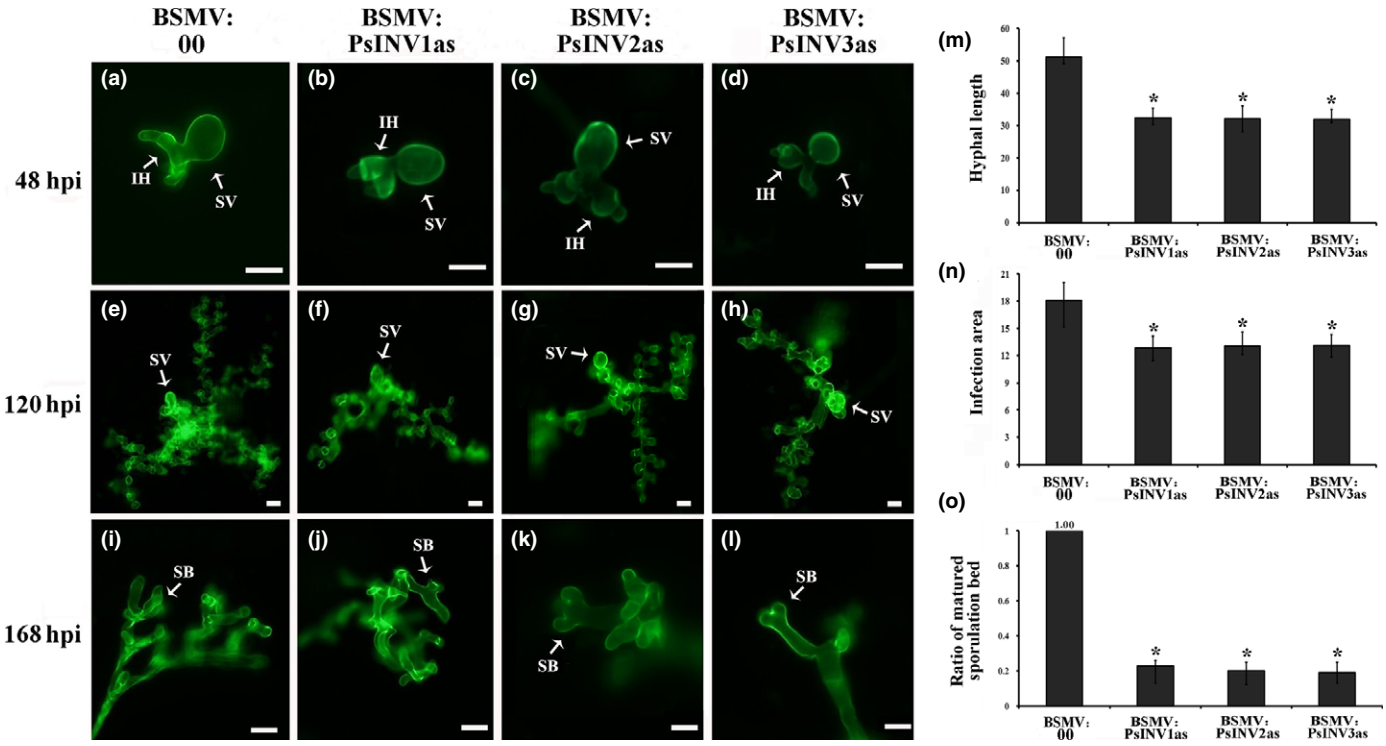

Fig. 8 Histological observation of fungal growth and development in wheat. Wheat leaves pre-inoculated with BSMV:00, BSMV:PsINV1as, BSMV:PsINV2as or BSMV:PsINV3as were sampled at (a–d) 48 h post-inoculation (hpi), (e–h) 120 hpi and (i–l) 168 hpi with *Pst* CYR32. After staining with wheatgerm agglutinin (WGA), fungal structure was examined under a fluorescence microscope. Bars, 20 μm. (m) Hyphal length (μm) was measured as the distance from the junction of the substomatal vesicle and the infection hypha to the tip of the infection hypha with DP-BSW software for the samples of 48 hpi . (n) Infection area (μm^2) was measured as the expanding hypha area with DP-BSW software (Olympus Corp.) for the samples of 120 hpi. (o) The ratio of matured sporulation bed was calculated by dividing the total sporulation bed number with the number of matured sporulation beds. All the statistical results were obtained from 50 infection sites per sporulation bed and values represent mean ± SE of three independent replicates. Differences were assessed using Student's *t*-tests. Asterisks indicate $P < 0.01$. SV, substomatal vesicle; IH, infection hypha; SB, sporulation bed.

© 2017 The Authors
New Phytologist © 2017 New Phytologist Trust

several domains enhance the efficiency of *Ps*INV to hydrolyze sucrose. The function of *Ps*INV in the *Pst* infection process was demonstrated by silencing the expression of *PsINV* using the HIGS system, as the pathogen invertase was shown to be indispensable for the pathogen growth and development.

The nutrient exchange zone for obligate fungi and host is the extrahaustorial matrix, a kind of specialized apoplast bordered by the haustorial plasma membrane and a modified cytoplasmic membrane of the host (extrahaustorial membrane); both membranes are fused at the 'neckband', which separates the extrahaustorial matrix from the bulk apoplast (Voegele & Mendgen, 2011; Garnica *et al.*, 2014). Some earlier studies showed that there is little protein present in the extrahaustorial membrane, so sucrose present in the extrahaustorial matrix is unlikely to be taken up by the host (Koh *et al.*, 2005; Voegele & Mendgen, 2011). It could be speculated that the pathogen plays an important role in the hydrolysis of sucrose in the extrahaustorial matrix. With a signal peptide confirmed for *Ps*INV, the enzyme is secreted, and may be responsible for the hydrolysis of sucrose in the extrahaustorial matrix and therefore render the pathogen independent of the host enzymatic machinery to secure its sugar demands (Siemens *et al.*, 2011).

Transcript profiling of *PsINV* also supports this hypothesis. The highest transcript levels of *PsINV* are observed during the crucial phase of the infection process, 72–168 hpi. This is the period when a high level of energy is required for *Pst* growth and development. After 168 hpi, transcript levels of *PsINV* decline again. This could be explained on the basis of the known stability of invertases. We speculated that it was because *Ps*INV was very stable as with other invertases, the amount of *Ps*INV produced with the extremely high expression between 72 and 168 hpi would be enough to persistently supply available sugar for *Pst* after 168 hpi in the compatible system . With entering the reproductive growth phase at 168 hpi, expression of *PsINV* decreased significantly. However, higher transcript levels were observed for a longer period in the incompatible systems, which is a more hostile environment for *Pst* as carbon and energy are limited due to the resistance reactions of the host. We speculate that there might be a feedback regulation in *Pst* for the lack of available sugar, so *PsINV* is more highly expressed in the incompatible systems to meet its carbon demands. With infection progressing, transcript levels of *PsINV* finally decreased to initial values. However, the significance of *PsINV* in the *Pst* infection process has been indicated by the high transcript levels in both compatible and incompatible systems.

The high transcript levels of the pathogen's invertase could play an important role in the observed increase of invertase activity at the infection site. Moreover, the particular structure of *Ps*INV could contribute to the increased invertase activity. A rust fungi-specific structure that is different from all other fungal invertases was uncovered by the prediction of functional domains. There are two GH32N domains in rust fungal invertases, but only one such domain in all other fungal invertases. A relationship between the rust fungi-specific structure and the higher efficiency for sucrose hydrolysis was identified in *Ps*INV. This would support a greater increase in invertase activity at infection sites. More importantly, it would provide the pathogen an advantage in the competition for photo-assimilates with the host (Bancal *et al.*, 2012). Pathogen invertases in infected tissue can therefore be considered a driving force in sugar unloading (together with the host invertases), and as a consequence, the normal carbohydrate transport in plants would be disturbed (Wright *et al.*, 1995; Ayres *et al.*, 1996; Lemoine *et al.*, 2013). In conclusion, our findings support the hypothesis that additional fungal

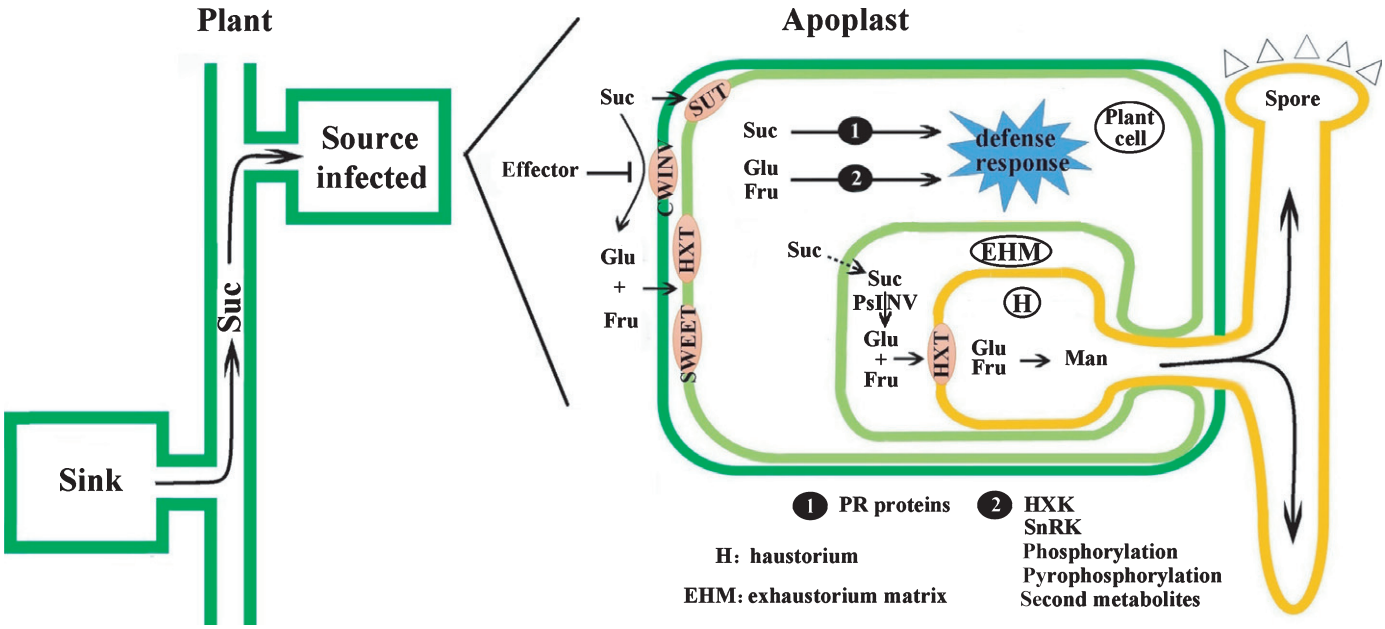

Fig. 9 Model depicting the effects of increased invertase activity. At the infection site, host (*Triticum aestivum*) invertase activity increases to induce the host defense response while the pathogen (*Puccinia striiformis* f. sp. *tritici*) invertase activity increases to meet its own carbon demands. With the increased sucrose demands, the initial source tissue infected by a pathogen is converted into a novel sink and sucrose transport is reallocated. Suc, sucrose; Glu, glucose; Fru, fructose; Man, mannitol; CWIN, cell-wall invertase; HXT, hexose transporter; SWEET, SWEET transporters.

© 2017 The Authors
New Phytologist © 2017 New Phytologist Trust

carbon demand in infected leaves converts original source tissue into another sink organ that competes with original sinks in the host, leading to a severe yield loss in the infected plants (Voegele *et al.*, 2006).

Like many sugar-cleaving enzymes (carbohydrate-active enzymes, CAZymes) from the glycoside hydrolase (GH) family that have been found to be highly expressed by pathogens during the infection process for successful invasion (Wu *et al.*, 2006; Ospina-Giraldo *et al.*, 2010; Takahashi *et al.*, 2013), *PsINV* is also highly expressed in the interaction with the host. Although invertases have been found in several plant pathogenic fungi, the importance of this kind of protein in the infection process is still unclear (Parrent *et al.*, 2009). To directly demonstrate the biological function of *PsINV* in the *Pst* infection process, HIGS was adopted as there are no stable genetic transformation methods for this obligate biotrophic fungus. Silencing *PsINV* resulted in suppression of growth and sporulation of *Pst*. Considering the biochemical function of *Ps*INV, it is likely that silencing *PsINV* inhibited hydrolysis of host sucrose, leading to a lack of available hexoses and eventually limited fungal growth and development. To our knowledge, this is the first direct *in vivo* evidence demonstrating that a pathogen's invertase plays a pivotal role in pathogenicity (Fig. 9). This is different from the hypothesis derived from the interaction between pathogenic bacteria and host in which the pathogen is believed to manipulate host cell-wall invertase for sucrose hydrolysis to absorb sugars (Ruan, 2014).

In conclusion, a highly conserved rust fungi-specific invertase, *Ps*INV, is abundantly secreted into the host to secure sugar absorption for *Pst*. It was shown that the pathogen invertase is essential for pathogen sugar absorption to support growth and development. Inhibition of pathogen glycoside hydrolases has been shown to be a part of the host defense system in a previous study (Choi *et al.*, 2013), and more recently, a GH12 family protein secreted in the host apoplast was recognized as a pathogen-associated molecular pattern (PAMP) (Ma *et al.*, 2015). Whether pathogen invertases have similar effects on the host defense response is unknown. As the function of the products of invertases, fructose and glucose can serve as signal molecules (Chiou & Bush, 1998; Gómez-Ariza *et al.*, 2007; Moghaddam & Ende, 2012), this is certainly a possibility, and further studies are needed on pathogen invertases.

Acknowledgements

This study was supported by the National Key Research and Development Program of China (2016YFD0100602), the National Key Basic Research Program of China (2013CB127700), the 111 Project of the Ministry of Education of China (B07049) and Chinese Universities Scientific Fund (2452017160).

Author contributions

Q.C., J.L. and Z.K. planned and designed the research. Q.C., X.L., S.H., Y.Y., D.L., L.C. and B.H. performed experiments and data analyses. Q.C., L.H., R.T.V. and Z.K. wrote the manuscript.

References

Ayres PG, Press MC, Spencer-Phillips PT. 1996. Effects of pathogens and parasitic plants on source–sink relationships. In: Zamski E, Schaffer AA, eds. *Photoassimilate distribution in plants and crops: source–sink relationships*. New York, NY, USA: Marcel Dekker, 479–499.

Bancal MO, Hansart A, Sache I, Bancal P. 2012. Modelling fungal sink competitiveness with grains for assimilates in wheat infected by a biotrophic pathogen. *Annals of Botany* **110**: 113–123.

Bradford MM. 1976. A rapid and sensitive method for the quantitation of microgram quantities of protein utilizing the principle of protein-dye binding. *Analytical Biochemistry* **72**: 248–254.

Cantu D, Govindarajulu M, Kozik A, Wang M, Chen X, Kojima KK, Jurka J, Michelmore RW, Dubcovsky J. 2011. Next generation sequencing provides rapid access to the genome of *Puccinia striiformis* f. sp. *tritici*, the causal agent of wheat stripe rust. *PLoS ONE* **6**: e24230.

Chang Q, Liu J, Wang Q, Han L, Liu J, Li M, Huang L, Yang J, Kang Z. 2013. The effect of *Puccinia striiformis* f. sp. *tritici* on the levels of water-soluble carbohydrates and the photosynthetic rate in wheat leaves. *Physiological and Molecular Plant Pathology* **84**: 131–137.

Chen WQ, Wu LR, Liu TG, Xu SC, Jin SL, Peng YL, Wang BT. 2009. Race dynamics, diversity, and virulence evolution in *Puccinia striiformis* f. sp. *tritici*, the causal agent of wheat stripe rust in China from 2003 to 2007. *Plant Disease* **93**: 1093–1101.

Cheng Y, Wang X, Yao J, Voegele RT, Zhang Y, Wang W, Huang L, Kang Z. 2015. Characterization of protein kinase *PsSRPKL*, a novel pathogenicity factor in the wheat stripe rust fungus. *Environmental Microbiology* **17**: 2601–2617.

Chiou TJ, Bush DR. 1998. Sucrose is a signal molecule in assimilate partitioning. *Proceedings of the National Academy of Sciences, USA* **95**: 4784–4788.

Choi HW, Kim NH, Lee YK, Hwang BK. 2013. The pepper extracellular xyloglucan-specific endo-β-1,4-glucanase inhibitor protein gene, *CaXEGIP1*, is required for plant cell death and defense responses. *Plant Physiology* **161**: 384–396.

Doidy J, Grace E, Kühn C, Simon-Plas F, Casieri L, Wipf D. 2012. Sugar transporters in plants and in their interactions with fungi. *Trends in Plant Science* **17**: 413–422.

Essmann J, Schmitz-Thom I, Schön H, Sonnewald S, Weis E, Scharte J. 2008. RNA interference-mediated repression of cell wall invertase impairs defense in source leaves of tobacco. *Plant Physiology* **147**: 1288–1299.

Finn RD, Coggill P, Eberhardt RY, Eddy SR, Mistry J, Mitchell AL, Potter SC, Punta M, Qureshi M, Sangrador-Vegas A *et al.* 2016. The Pfam protein families database: towards a more sustainable future. *Nucleic Acids Research* **44**: D279–D285.

Garnica DP, Nemri A, Upadhyaya NM, Rathjen JP, Dodds PN. 2014. The ins and outs of rust haustoria. *PLoS Pathogens* **10**: e1004329.

Ghose TK. 1987. Measurement of cellulase activities. *Pure & Applied Chemistry* **59**: 257–268.

Gómez-Ariza J, Campo S, Rufat M, Estopà M, Messeguer J, Segundo BS, Coca M. 2007. Sucrose-mediated priming of plant defense responses and broad-spectrum disease resistance by overexpression of the maize pathogenesis-related PRms protein in rice plants. *Molecular Plant–Microbe Interactions* **20**: 832–842.

Gu B, Kale SD, Wang Q, Wang D, Pan Q, Cao H, Meng Y, Kang Z, Tyler BM, Shan W. 2011. Rust secreted protein Ps87 is conserved in diverse fungal pathogens and contains a RXLR-like motif sufficient for translocation into plant cells. *PLoS ONE* **6**: e27217.

Guenther JC, Hallen-Adams HE, Bücking H, Shachar-Hill Y, Trail F. 2009. Triacylglyceride metabolism by *Fusarium graminearum* during colonization and sexual development on wheat. *Molecular Plant–Microbe Interactions* **22**: 1492–1503.

Hayes MA, Feechan A, Dry IB. 2010. Involvement of abscisic acid in the coordinated regulation of a stress-inducible hexose transporter (VvHT5) and a cell wall invertase in grapevine in response to biotrophic fungal infection. *Plant Physiology* **153**: 211–221.

© 2017 The Authors
New Phytologist © 2017 New Phytologist Trust

Holzberg S, Brosio P, Gross C, Pogue GP. 2002. *Barley stripe mosaic virus*-induced gene silencing in a monocot plant. *Plant Journal* **30**: 315–327.

Hood ME, Shew HD. 1996. Applications of KOH-aniline blue fluorescence in the study of plant–fungal interactions. *Phytopathology* **86**: 704–708.

Käll L, Krogh A, Sonnhammer EL. 2007. Advantages of combined transmembrane topology and signal peptide prediction – the Phobius web server. *Nucleic Acids Research* **35**: W429–W432.

Kelley LA, Mezulis S, Yates CM, Wass MN, Sternberg MJ. 2015. The Phyre2 web portal for protein modeling, prediction and analysis. *Nature Protocols* **10**: 845–858.

Koch K. 2004. Sucrose metabolism: regulatory mechanisms and pivotal roles in sugar sensing and plant development. *Current Opinion in Plant Biology* **7**: 235–246.

Koh S, André A, Edwards H, Ehrhardt D, Somerville S. 2005. *Arabidopsis thaliana* subcellular responses to compatible *Erysiphe cichoracearum* infections. *Plant Journal* **44**: 516–529.

Lemoine R, La Camera S, Atanassova R, Dédaldéchamp F, Allario T, Pourtau N, Bonnemain J-L, Laloi M, Coutos-Thévenot P, Maurousset L. 2013. Source-to-sink transport of sugar and regulation by environmental factors. *Frontiers in Plant Science* **4**: 272.

Li L, Zhao C, Li H, Li W, Zhang L, Xu D, Wang J, Li H. 2011. Establishment of the plasmid standard curve generation method for absolute quantification PCR. *Journal of Agricultural Biotechnology* **19**: 1157–1162.

Liu J, Han L, Huai B, Zheng P, Chang Q, Guan T, Li D, Huang L, Kang Z. 2015. Down-regulation of a wheat alkaline/neutral invertase correlates with reduced host susceptibility to wheat stripe rust caused by *Puccinia striiformis*. *Journal of Experimental Botany* **66**: 7325–7338.

Livak KJ, Schmittgen TD. 2001. Analysis of relative gene expression data using real-time quantitative PCR and the $2^{-\Delta\Delta CT}$ method. *Methods* **25**: 402–408.

Long DE, Fung AK, McGee EEM, Cooke RC, Lewis DH. 1975. The activity of invertase and its relevance to the accumulation of storage polysaccharides in leaves infected by biotrophic fungi. *New Phytologist* **74**: 173–182.

Ma Z, Song T, Zhu L, Ye W, Wang Y, Shao Y, Dong S, Zhang Z, Dou D, Zheng X. 2015. A *Phytophthora sojae* glycoside hydrolase 12 protein is a major virulence factor during soybean infection and is recognized as a PAMP. *Plant Cell* **27**: 2057–2072.

Miller GL. 1959. Use of dinitrosalicylic acid reagent for determination of reducing sugar. *Analytical Chemistry* **31**: 426–428.

Moghaddam MRB, Ende WVd. 2012. Sugars and plant innate immunity. *Journal of Experimental Botany* **63**: 3989–3998.

Nirmala J, Tom D, Lawrence PK, Yin C, Hulbert S, Steber CM, Steffenson BJ, Szabo LJ, von Wettstein D, Kleinhofs A. 2011. Concerted action of two avirulent spore effectors activates reaction to *Puccinia graminis* 1 (*Rpg1*)-mediated cereal stem rust resistance. *Proceedings of the National Academy of Sciences, USA* **108**: 14676–14681.

Nowara D, Gay A, Lacomme C, Shaw J, Ridout C, Douchkov D, Hensel G, Kumlehn J, Schweizer P. 2010. HIGS: host-induced gene silencing in the obligate biotrophic fungal pathogen *Blumeria graminis*. *Plant Cell* **22**: 3130–3141.

Ospina-Giraldo MD, Griffith JG, Laird EW, Mingora C. 2010. The CAZyome of *Phytophthora* spp.: a comprehensive analysis of the gene complement coding for carbohydrate-active enzymes in species of the genus *Phytophthora*. *BMC Genomics* **11**: 525.

Panwar V, McCallum B, Bakkeren G. 2013. Host-induced gene silencing of wheat leaf rust fungus *Puccinia triticina* pathogenicity genes mediated by *Barley stripe mosaic virus*. *Plant Molecular Biology* **81**: 595–608.

Parrent J, James TY, Vasaitis R, Taylor AF. 2009. Friend or foe? Evolutionary history of glycoside hydrolase family 32 genes encoding for sucrolytic activity in fungi and its implications for plant-fungal symbioses. *BMC Evolutionary Biology* **9**: 148.

Petersen TN, Brunak S, Gv Heijne, Nielsen H. 2011. SignalP 4.0: discriminating signal peptides from transmembrane regions. *Nature Methods* **8**: 785–786.

Price NC. 1985. The determination of K_m values from Lineweaver–Burk plots. *Biochemical Education* **13**: 81.

Roitsch T, Balibrea M, Hofmann M, Proels R, Sinha A. 2003. Extracellular invertase: key metabolic enzyme and PR protein. *Journal of Experimental Botany* **54**: 513–524.

Roitsch T, González MC. 2004. Function and regulation of plant invertases: sweet sensations. *Trends in Plant Science* **9**: 606–613.

Ruan Y-L. 2012. Signaling role of sucrose metabolism in development. *Molecular Plant* **5**: 763–765.

Ruan Y-L. 2014. Sucrose metabolism: gateway to diverse carbon use and sugar signaling. *Annual Review of Plant Biology* **65**: 33–67.

Ruffner HP, Geissmann M, Rast DM. 1992. Plant and fungal invertases in grape berries infected with *Botrytis cinerea*. *Physiological and Molecular Plant Pathology* **40**: 181–189.

Ruiz E, Ruffner HP. 2002. Immunodetection of *Botrytis*-specific invertase in infected grapes. *Journal of Phytopathology* **150**: 76–85.

Scholes JD, Lee PJ, Horton P, Lewis DH. 1994. Invertase: understanding changes in the photosynthetic and carbohydrate metabolism of barley leaves infected with *Powdery Mildew*. *New Phytologist* **126**: 213–222.

Senthil-Kumar M, Hema R, Anand A, Kang L, Udayakumar M, Mysore KS. 2007. A systematic study to determine the extent of gene silencing in *Nicotiana benthamiana* and other Solanaceae species when heterologous gene sequences are used for virus-induced gene silencing. *New Phytologist* **176**: 782–791.

Sherman F. 1991. Getting started with yeast. *Methods in Enzymology* **194**: 21.

Siemens J, Gonzalez MC, Wolf S, Hofmann C, Greiner S, Du Y, Rausch T, Roitsch T, Muller J. 2011. Extracellular invertase is involved in the regulation of clubroot disease in *Arabidopsis thaliana*. *Molecular Plant Pathology* **12**: 247–262.

Smeekens S, Ma J, Hanson J, Rolland F. 2010. Sugar signals and molecular networks controlling plant growth. *Current Opinion in Plant Biology* **13**: 273–278.

Swarbrick PJ, Schulze-Lefert P, Scholes JD. 2006. Metabolic consequences of susceptibility and resistance (race-specific and broad-spectrum) in barley leaves challenged with powdery mildew. *Plant, Cell & Environment* **29**: 1061–1076.

Takahashi M, Yoshioka K, Imai T, Miyoshi Y, Nakano Y, Yoshida K, Yamashita T, Furuta Y, Watanabe T, Sugiyama J. 2013. Degradation and synthesis of β-glucans by a *Magnaporthe oryzae* endotransglucosylase, a member of the glycoside hydrolase 7 family. *Journal of Biological Chemistry* **288**: 13821–13830.

Tamura K, Peterson D, Peterson N, Stecher G, Nei M, Kumar S. 2011. MEGA5: molecular evolutionary genetics analysis using maximum likelihood, evolutionary distance, and maximum parsimony methods. *Molecular Biology & Evolution* **28**: 2731–2739.

Tang X, Rolfe SA, Scholes JD. 1996. The effect of *Albugo candida* (white blister rust) on the photosynthetic and carbohydrate metabolism of leaves of *Arabidopsis thaliana*. *Plant, Cell & Environment* **19**: 967–975.

Thompson JD, Higgins DG, Gibson TJ. 1994. CLUSTAL W: improving the sensitivity of progressive multiple sequence weighing, position-specific gap penalties and weight matrix choice. *Nucleic Acids Research* **22**: 4673–4680.

Voegele RT, Mendgen KW. 2011. Nutrient uptake in rust fungi: how sweet is parasitic life? *Euphytica* **179**: 41–55.

Voegele RT, Wirsel S, Möll U, Lechner M, Mendgen K. 2006. Cloning and characterization of a novel invertase from the obligate biotroph *Uromyces fabae* and analysis of expression patterns of host and pathogen invertases in the course of infection. *Molecular Plant-Microbe Interactions* **19**: 625–634.

Wahl R, Wippel K, Goos S, Kämper J, Sauer N. 2010. A novel high-affinity sucrose transporter is required for virulence of the plant pathogen *Ustilago maydis*. *PLoS Biology* **8**: 435.

Wang CF, Huang LL, Buchenauer H, Han QM, Zhang HC, Kang ZS. 2007. Histochemical studies on the accumulation of reactive oxygen species (O^{2-} and H_2O_2) in the incompatible and compatible interaction of wheat-*Puccinia striiformis* f. sp. *tritici*. *Physiological & Molecular Plant Pathology* **71**: 230–239.

Wellings CR. 2011. Global status of stripe rust: a review of historical and current threats. *Euphytica* **179**: 129–141.

Wright DP, Baldwin BC, Shephard MC, Scholes JD. 1995. Source–sink relationships in wheat leaves infected with powdery mildew. I. Alterations in carbohydrate metabolism. *Physiological and Molecular Plant Pathology* **47**: 237–253.

© 2017 The Authors
New Phytologist © 2017 New Phytologist Trust

Wu SC, Halley JE, Luttig C, Fernekes LM, Gutiérrez-Sanchez G, Darvill AG, Albersheim P. 2006. Identification of an endo-β-1, 4-D-xylanase from *Magnaporthe grisea* by gene knockout analysis, purification, and heterologous expression. *Applied and Environmental Microbiology* **72**: 986–993.

Zhang X, Han D, Zeng Q, Duan Y, Yuan F, Shi J, Wang Q, Wu J, Huang L, Kang Z. 2013. Fine mapping of wheat stripe rust resistance gene *Yr26* based on collinearity of wheat with *Brachypodium distachyon* and rice. *PLoS ONE* **8**: e57885.

Zhang Y, Qu Z, Zheng W, Liu B, Wang X, Xue X, Xu L, Huang L, Han Q, Zhao J. 2008. Stage-specific gene expression during urediniospore germination in *Puccinia striiformis* f. sp *tritici*. *BMC Genomics* **9**: 203.

Zheng W, Huang L, Huang J, Wang X, Chen X, Zhao J, Guo J, Zhuang H, Qiu C, Liu J. 2013. High genome heterozygosity and endemic genetic recombination in the wheat stripe rust fungus. *Nature Communications* **4**: 2673.

Supporting Information

Additional Supporting Information may be found online in the Supporting Information tab for this article:

Fig. S1 Sequences of *PsINV* from different races analyzed for intraspecies polymorphism.

Fig. S2 cDNA from the incompatible system used for qRT-PCR.

Fig. S3 The eukaryotic expression product of *Ps*INV as identified by SDS-PAGE and Western blot.

Fig. S4 The proteins used for invertase activity tests as verified by Western blot.

Fig. S5 The three fragments used for silencing *PsINV* selected without mistargeting.

Fig. S6 Standard curves generated for the absolute quantification of *Pst* and wheat, respectively.

Table S1 The primers used in this study

Table S2 Statistical analysis of fungal growth in wheat leaves inoculated with BSMV at 24 hpi

Please note: Wiley Blackwell are not responsible for the content or functionality of any Supporting Information supplied by the authors. Any queries (other than missing material) should be directed to the *New Phytologist* Central Office.

About *New Phytologist*

- *New Phytologist* is an electronic (online-only) journal owned by the New Phytologist Trust, a **not-for-profit organization** dedicated to the promotion of plant science, facilitating projects from symposia to free access for our Tansley reviews.
- Regular papers, Letters, Research reviews, Rapid reports and both Modelling/Theory and Methods papers are encouraged. We are committed to rapid processing, from online submission through to publication 'as ready' via *Early View* – our average time to decision is <26 days. There are **no page or colour charges** and a PDF version will be provided for each article.
- The journal is available online at Wiley Online Library. Visit **www.newphytologist.com** to search the articles and register for table of contents email alerts.
- If you have any questions, do get in touch with Central Office (np-centraloffice@lancaster.ac.uk) or, if it is more convenient, our USA Office (np-usaoffice@lancaster.ac.uk)
- For submission instructions, subscription and all the latest information visit **www.newphytologist.com**

© 2017 The Authors
New Phytologist © 2017 New Phytologist Trust